Chapter 7

Types of cavitation: VISCOUS EFFECTS ON INCEPTION OF SHEET CAVITATION

Objective: *Description of the effects of the boundary layer on inception of sheet cavitation.*

Cavitation inception takes place when nuclei are exposed to a pressure lower than the critical pressure. But the minimum pressure around a foil or propeller blade occurs on or close to a solid surface, where a boundary layer exists. This boundary layer has an effect on the pressures encountered by the nuclei. These effects are summarized as viscous effects on cavitation inception, because the boundary layer is a viscous phenomenon.

Figure 7.1: The pressure distribution on a foil with natural transition to turbulence

7.1 Inception at the transition location

The blade sections of a ship propeller are thin and the minimum pressure occurs at the leading edge with strong gradients, both favorable (upstream of the minimum pressure point) and adverse (downstream of the minimum pressure point). At the stagnation point the boundary layer begins laminar, and after some distance transition to turbulence takes place. The location of transition depends on the flow velocity (the local Reynolds number $Rn = \frac{V.s}{\nu}$, where s is the distance along the body from the stagnation point). An adverse pressure gradient stimulates transition and therefore it will often take place downstream of the location of minimum pressure. This situation is sketched in Fig 7.1.

This pressure distribution will generally lead

to sheet cavitation when the minimum pressure is lower than the critical pressure of the nuclei in the flow. Sheet cavitation means that the growing cavition bubbles induce separation of the flow and the cavitation becomes attached to the foil over a certain length (see chapter 6). However, when the pressure is between the minimum pressure and the pressure at the transition location, *no cavitation will occur*. When the pressure is lowered until below the transition pressure, cavitation inception is found at the pressure in the transition location [1].

On propellers the low pressure peak at the leading edge is often sharp, and the locations of minimum pressure and transition are very close together and difficult to distinguish.A simple body with an attached boundary layer without laminar separation (like on the hemispherical headform) is the cylindrical Schiebe body (see Appendix B. At model scale Reynolds numbers the transition region from laminar to turbulent can better be distinguished from the minimum pressure location.

7.1.1 Boundary Layer Transition

Transition is a complicated process, which is not yet properly understood or described. This is the same for turbulence. Their main features, relevant for cavitation research, are briefly mentioned below.

In a turbulent flow the velocitie $u(t)$ in a certain location in a certain direction consists of a mean velocity $\bar{u}$ and a component u' which varies in time. The turbulence in that direction is then defined as $\frac{1}{T}\sqrt{\int_0^T u'^2 dt}$. The temporal velocity components u' are assumed to be chaotic and therefore have a stochastic behavior. When in a flow all three velocity components have the same magnitude the turbulence is called homogeneous and the turbulence level is $\frac{1}{T}\sqrt{\int_0^T (u'^2 + v'^2 + w'^2)dt}$ where u, v and w are the three velocity components. The pressure in a turbulent flow also exhibits temporal variations, so $p(t) = \bar{p} + p'(t)$. However, in a boundary layer the turbulence is not homogeneous and may consist of more deterministic isolated vortex structures and the minimum pressure in the boundary layer may depend on the minimum pressure in the hairpin vortices.

Transition to turbulence occurs when a laminar boundary layer with a certain velocity profile develops into a turbulent boundary layer with a turbulent velocity profile. In boundary layers the first stage of transition is the amplification of small disturbances from the flow (flow turbulence) or from the wall (roughness). Since the disturbances are small they behave linearly. In *two dimensional* boundary layers transition can be indicated by the linear stability of the boundary layer. Starting at the laminar Navier Stokes equations the laminar boundary layer equations are found by linearizing all terms perpendicular to the wall. Then the velocities and the pressure are split into a mean and a time varying part, as described above. The time varying part is written as a Fourier series in the form of $u' = u_1 e^{i\omega(x-ct)}$. This leads to the "Orr-Sommerfeld equations" for the disturbance velocities. From stability considerations it follows that only a small range of frequencies ω are amplified. This leads to a wave-like disturbance of the boundary layer, the so-called *Tollmien-Schlichting* waves. These waves are rapidly amplified and they result in three-dimensional instabilities, which by viscous decay develop into turbulence. A simple criterion used for the definition of transition is the magnification factor of an initial disturbance. This magnification factor can be calculated from the Orr-Sommerfeld equations for each possible disturbance fre-

quency. The frequency which is amplified most is the frequency which is considered crucial for turbulence. An often used criterion for transition, based on experimental data, is the value e^9. The initial disturbance is then amplified more than 8000 times. Amplification of a disturbance depends strongly on the pressure distribution. A favorable pressure gradient will damp the disturbances and delay transition, an adverse pressure gradient will stimulate the magnification of disturbances and stimulate transition. For details see a handbook such as Schlichting ([44]).

When the mean pressure in Fig. 7.1 is lowered until the pressure at the transition location approaches the vapor pressure, cavitation will occur in the form of small local bubbles. But when the pressure gradient in the transition region is strong a sudden sheet cavity may occur. This can be explained by the fact that in the transition region strong pressure fluctuations occur. The minimum pressure is lower than the vapor pressure and nuclei passing through that region may reach their critical pressure and expand into bubbles. Depending on the pressure gradient these bubbles may move with the flow in the boundary layer and collapse or they may expand upstream and downstream to form a sheet cavity.

The important aspects of this short description of turbulent transition for cavitation inception are:

- The location of transition is not a single location, but a range. The length of this range depends on the pressure distribution.

- Transition requires an initial disturbance such as flow turbulence. However, the effectiveness of a disturbance depends strongly on the frequency.

- The location of transition depends on the Reynolds number. With increasing Reynolds number the transition location will move upstream.

- The location of transition depends strongly on the pressure distribution. An adverse pressure distribution will stimulate transition. On a foil transition will therefore occur downstream of the minimum pressure location.

7.2 Inception at a Separation Bubble

Another common situation of the boundary layer on a foil is sketched in Fig. 7.2. From the stagnation point the boundary layer is laminar, but downstream of the minimum pressure point the adverse pressure gradient is so strong that the boundary layer separates. The separated surface is very unstable and will become turbulent after a short time. The turbulent free surface will reattach the boundary layer to the wall, but after reattachment the boundary layer is turbulent. The separation bubble is a small region of constant pressure. When the pressure gradient is very high a long separation bubble may occur, but this is not very common on foils.

When the mean pressure is lowered so that the minimum pressure is below the vapor pressure again no cavitation will occur due to bubble screening. The very sharp minimum pressure peak will make the effect of screening even stronger. Only when the pressure at the re-attachment region will reach the vapor pressure inception will take place. In some cases on a Schiebe headform the inception could be localized as small bubbles in the re-attachment zone. But when the pressure is lowered only slightly the cavity becomes a small sheet cavity, because the vapor fills the separation bubble. Further lowering of the pressure will increase the length of the sheet
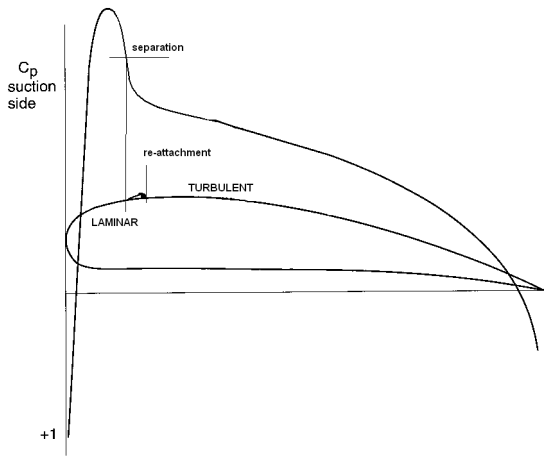
Figure 7.2: The pressure distribution on a foil with a laminar separation bubble

cavity.

Figure 7.3: Cavitation on a propeller blade with laminar flow and local separation

7.3 Examples

At model scale there is cavitation inception when there is a laminar separation bubble at the leading edge, and no inception when the boundary layer in the low pressure region remains laminar. An example of the described phenomena on a model propeller is shown in Fig 7.3. This is a propeller with an unloaded tip, so the tip vortex cavitation is small. The maximum loading is at 0.7R. But there is no cavitation at that radius. The only cavitation is in a small region between 0.8R and 0.9R. The extreme length of the cavity there illustrates that the minimum pressure at the blade leading edge is far below the vapor pressure. The shape of the leading edge sheet at the leading edge indicates that there is separation at the leading edge, probably caused by the shape of the leading edge.

In commercial ship propellers, where the tip loading is not strongly reduced, the low pres-sure peak occurs at the outer radii of the pro-peller. At model scale the inner part of the sheet may then be absent, as shown in Fig. 7.4. At the outer radii there is extensive sheet cav-itation, caused by laminar separation at the leading edge. At inner radii there is no cav-itation. The minimum pressure there is very much below the vapor pressure, but there is no inception!

7.4 Reynolds Effects on Inception of Sheet Cavitation

Scale effects are defined as differences between model and full scale. Since it is expected that cavitation inception at full scale occurs at the vapor pressure, scale effects on inception can also be defined as deviations of the inception pressure from the vapor pressure. Since viscous scale effects are caused by a lower Reynolds number at model scale, the
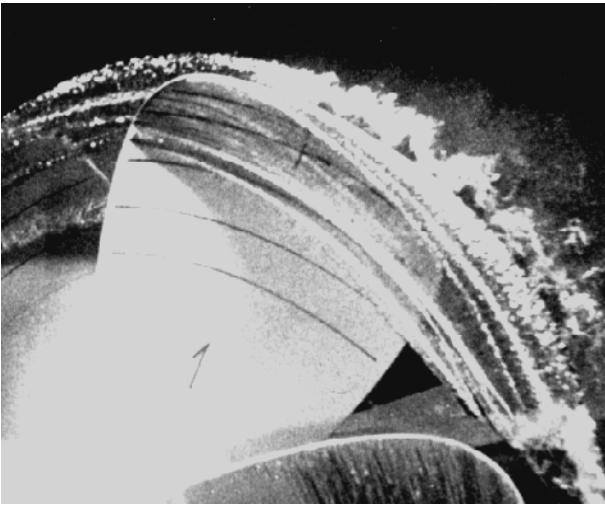
Figure 7.4: Sheet cavitation at laminar separation

usual method to reduce these scale effects is to increase the Reynolds number of the model tests. This also has the effect that smaller nuclei are required. In a cavitation tunnel the increase of the Reynolds number is limited by the maximum tunnel velocity or by the forces generated by increased tunnel velocity. When a free surface is present there is no choice and the Reynolds number is determined because the Froude number is maintained. Based on flat plate results the ITTC has recommended some time to do cavitation tests with a minimum Reynolds number based on the propeller chord of $2*10^5$.

An increase of the Reynolds number will move the transition region, as observed in Fig. 8.2, towards the leading edge. However, transition is not only determined by the Reynolds number, but also by the pressure distribution. The result of a paint test at high Reynolds number on the paint pattern of a propeller is shown in Fig. 7.5. (Reynolds number at 0.7R based on chordlength and local inflow velocity is $6*10^6$!). The minimum pressure in this condition is in the midchord region. At a lower Reynolds number transi-

tion occurred in the midchord region over the whole propeller blade ([34]). An increase of the Reynolds number moves the transition region towards the leading edge, but it remains far away from it. What is observed is the occurrence of turbulent spots. These spots originate on a fixed location on the blade and caused by small surface irregularities. The surface irregularities become effective when the boundary layer becomes thinner at higher Reynolds numbers.

The effect of turbulent streaks on cavitation inception is the occurrence of cavitation spots, as shown in Fig. 7.6 in the region where no sheet cavitation is present due to a laminar boundary layer. Generally such a region of spots occurs at inner radii of a sheet cavity, as shown in Fig. 7.9. Detailed observations of such cavitation spots on a foil with varying pressure are shown in Figs. 7.7 and 7.8.

An increase in Reynolds number makes the boundary layer more susceptible to surface irregularities, which result in turbulent streaks in a laminar boundary layer. Such streaks do not only affect sheet cavitation inception, but also the inception and occurrence of bubble cavitation. An effect of such a turbulent spot on bubble cavitation is shown in Fig. 7.10. The minimum pressure on this blade is in the midchord region and the pressure in that region is below the vapor pressure. There is little or no bubble cavitation due to a lack of nuclei. however, at certain spots, which coincided with turbulent streaks in the paint test, bubble cavitation is visible. An increase in nuclei increases the occurrence of traveling bubble cavitation in the midchord region, as shown in Fig. 7.11, but the spot remains unchanged. In Fig.7.10 the spot of bubble cavitation has a sharp peak, indicating that the surface irregularity which causes the spot is located in the origin of the spot. This is not necessarily so. The surface irregularity
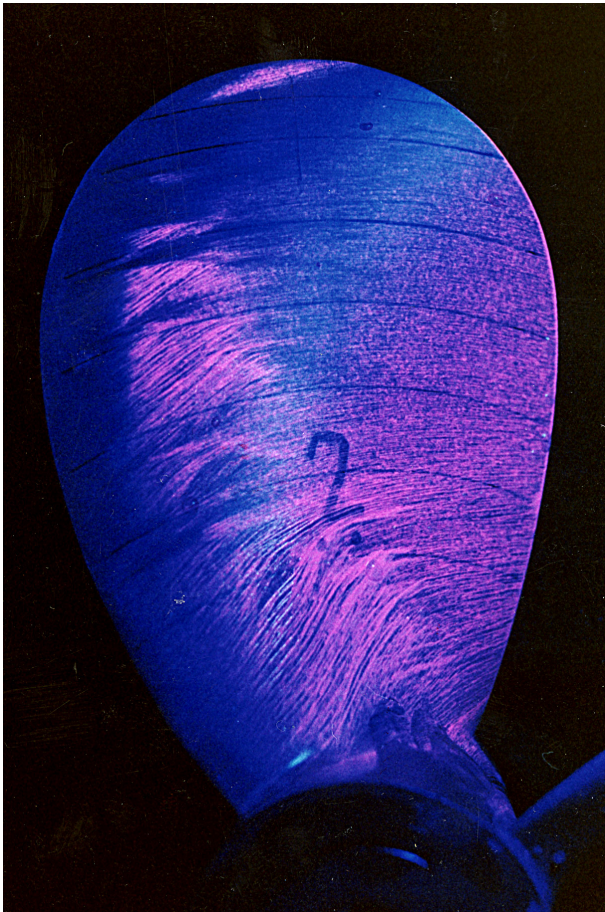
Figure 7.5: Paint pattern at high Reynolds number

which creates the turbulent spot may be far upstream of the low pressure region. This will still result in inception of bubble cavitation in the low pressure region, but with a less pointed spot, as shown in Fig. 7.12

7.5   Reynolds Effects on the inception of vortex cavitation

attached and detached vortex cavitation. Relation with boundary layer.
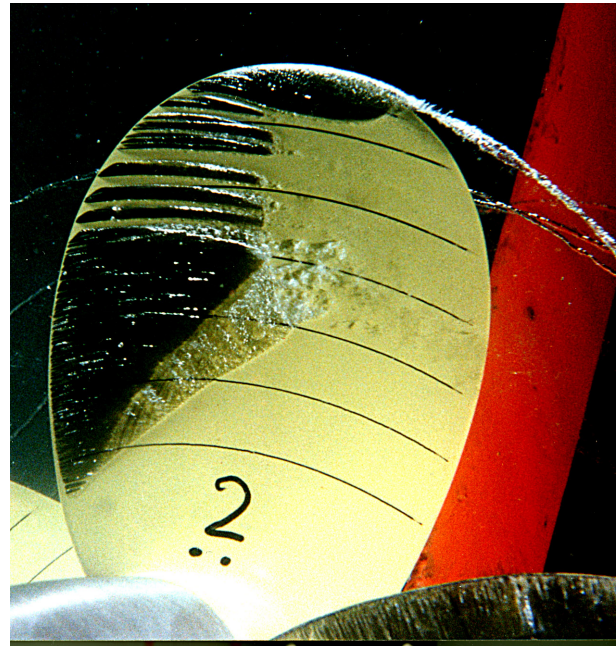
Figure 7.6: Cavitation Spots due to surface irregularities

7.6   Nuclei and Viscous Effects

To complicate the phenomena observed in this section it has to be kept in mind that cavitation inception caused by laminar separation or by turbulent boundary layers still requires nuclei. It is possible to suppress these effects when the nuclei content is very low, as occurs e.g. in a depressurized towing tank after a long standing time (weekends). It seems that the viscous effects mentioned here only *decrease* the required size of the nuclei. And since smaller nuclei are more abundant than larger ones, inception due to viscous effects is less sensitive to the nuclei content. So it is possible that sheet cavitation in a region with laminar separation is absent due to a very low nuclei content. Electrolysis will then be effective. An example is the observation of a propeller in the Marin Depressurized Towing Tank, given in Fig. 7.13. There is no sheet cavitation on this blade,
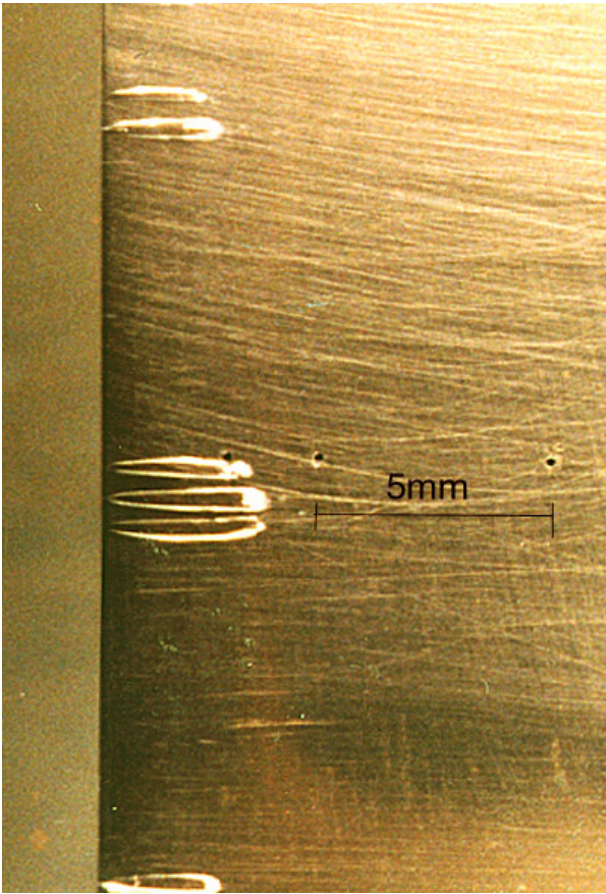
Figure 7.7: Cavitation spot near inception
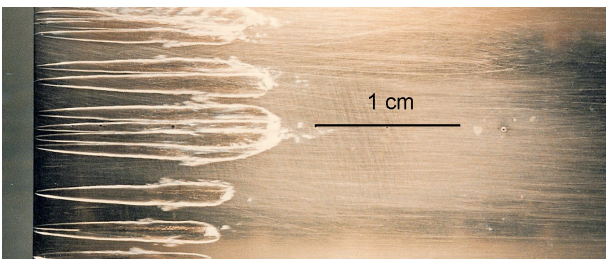
Figure 7.8: Developed cavitation spot

but when electrolysis was applied the sheet appeared (Fig. 7.14). Still from the structure of the sheet it is visible that it originates at a separation bubble because of its smooth surface. Moreover, the spots at the inner radii reveal laminar flow effects. Especially the occurrence of cavitation spots as in Fig. 7.7 is often found to be stimulated by additional
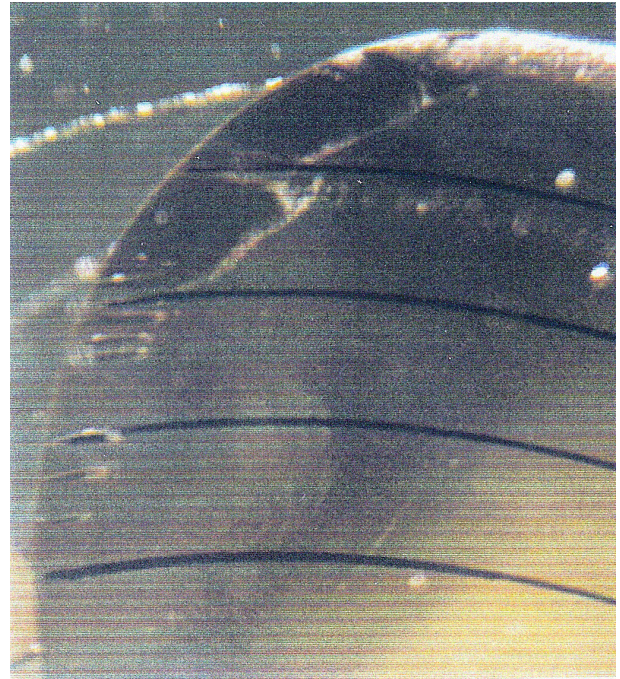
Figure 7.9: Spots of cavitation in the inner region of a sheet cavity

Figure 7.10: Bubble cavitation due to a turbulent spot

Figure 7.11: Bubble cavitation due to a turbulent spot with electrolysis
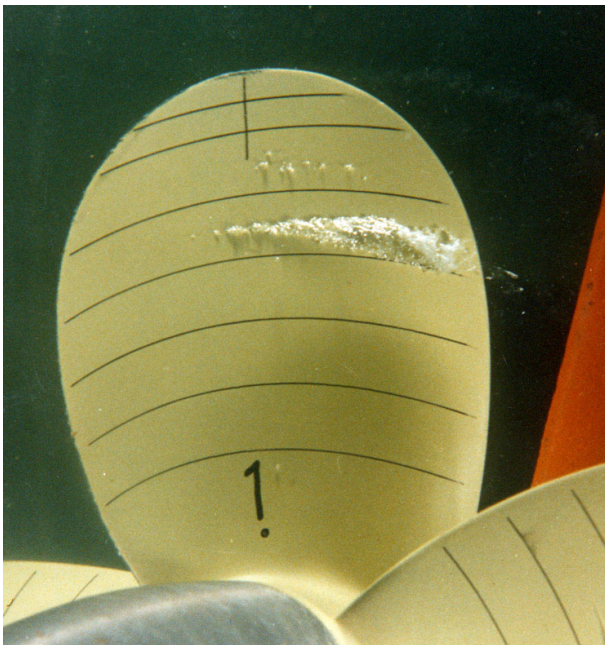
Figure 7.12: Bubble cavitation due to a turbulent spot with electrolysis
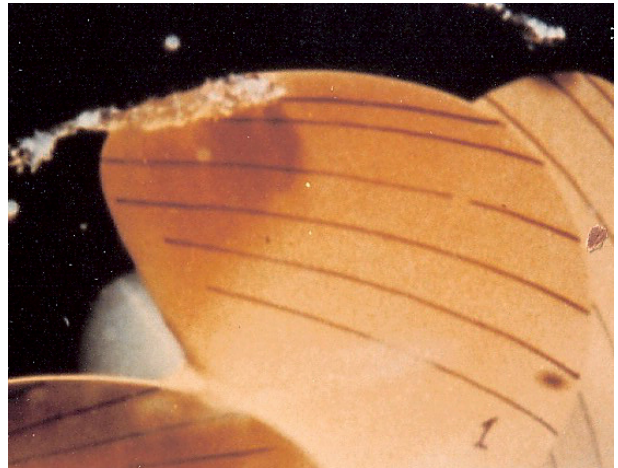
Figure 7.13: Propeller observation in the Depressurized Towing Tank without electrolysis

Figure 7.14: Propeller observation in the Depressurized Towing Tank without electrolysis

nuclei. Similarly it is possible to distinguish from the structure of the bubble cavities in Fig. 7.11 if the origin of the cavitation is in free stream nuclei or in surface generated nuclei.

The explanation of the phenomena observed can only be described tentatively. Inception at the reattachment point of a laminar separation bubble and in the transition region of a boundary layer has been attributed to local low pressures in those regions. This would mean that

small nuclei, which will not reach their critical size in the mean flow, experience a lower pressure locally and will grow. Wall pressure fluctuations have been measured in the boundary layer, but the pressures in the vortical structures may be lower than the wall pressures. Another element is the mixing effect of turbulent boundary layers, which causes nuclei from the outer flow to be transported towards the wall, where the local velocity is lower and the residence time is longer. In laminar separation bubbles nuclei can even be trapped for a longer time and grow or coalesce with other nuclei. From the Reynolds effects it became clear that surface irregularities not only cause inception, bit also that they were a source of nuclei which could seed bubble cavitation downstream. Apparently local surface irregularities create local low pressures on a micro scale which in turn generate nuclei. The free stream turbulence will also affect transition and indirectly inception. It is known that an increase of the turbulence level in a cavitation tunnel stimulates inception [29]. On the other hand, when a model propeller operates in the turbulent wake of a model, laminar boundary layers occur frequently and the turbulence is unable to cause transition on the propeller blades. Apparently the scale of the turbulence is also important.

When not only the minimum pressure is involved, but also pressure fluctuations in the boundary layer, even more mechanisms come into play such as the resonance frequency of the nuclei and rectified diffusion, which may cause growth of nuclei.

It is also known that nuclei can also affect the boundary layer and stimulate transition, especially when they are embedded in the boundary layer.

All this is not well understood, and certainly not quantified. The structure of turbulence in transition and separation is a topic in fluid dynamics that is still being explored. This makes that in cavitation inception after the fact there are always factors that may tentatively explain what happened. But prediction remains very difficult.

Bibliography

[1] Arakeri,V.H., Acosta, A.J., 1979, *Viscous Effects in the Inception of Cavitation*, A.S.M.E. Int. Symposium on Cavitation, New York, USA.

[2] Arndt, R.E.A., 1976, *Cavitation on Model Propellers with Boundary Layer Trips*, A.S.M.E.Conference on Polyphase Flow, New Orleans, USA.

[3] Arndt, R.E.A., Ellis, C.R., Paul, S. 1995, *Preliminary Investigation of the Use of Air Injection to mitigate Cavitation Erosion*, A.S.M.E. Journal of Fluids Engineering, Vol.117.

[4] Briggs, L.J., 1950 *Limiting negative pressure of water.*, J. Applied Phys. 21:721722.

[5] Brennen, C.E., 1995 *Cavitation and Bubble Dynamics*, Oxford University Press, ISBN 0-19-509409-3. Also available on internet.

[6] Burrill, L.C., 1951, *Sir Charles Parsons and Cavitation*, Transactions of the Institute of Marine Engineers.

[7] Borkent, B.M., 2009, *Interfacial Phenomena in Micro- and Nanofluidics: nanobubbles,cavitation, and wetting*, Thisis Twente University, The Netherlands.

[8] Coutier-Delgosha, O., Devillers, J-P., Leriche, M., Pichon, T., 2005, emphEffect of Roughness on the Dynamics of Unsteady Cavitation, Journal of Fluids Eng. , vol 127.

[9] Epstein, P.S., Plesset, M.S. 1950 *On the stability of Gas Bubbles in Liquis-Gas Solutions*, Journal of Chemical Physics, Vol.18., pp1505-1509.

[10] , Feindt, E.G., 1956,*Untersuchungen uber die Abhangigkeit des Umschlages Laminar-Turbulent von der Oberflachenrauhigkeit und der Druckverteilung*, Jahrbuch STG, Bd.50, pp180-205

[11] Flynn, H.G., 1964, *Physics of Acoustic Cavitation*, W.P.Mason ed. Vol1,PartB,Academic Press New York-London.

[12] Foeth, E-J., Kuiper, G. 2004, *Exploratory experiments to determine flow and structure borne noise of erosive cavity implosions*, A¿S¿M¿E¿ Fluids Eng. Summer Conference, HT-FED2004-56789, Charlotte, NC. USA.

[13] Foeth, E-J., *The Structure of Three-Dimensional Sheet Cavitation*, Thesis Technical University Delft.

[14] Fox, F.E., Herzfeld, K.F., 1954 *Gas Bubbles with Organic Skin as Cavitation Nuclei*, J.Acoust. Soc. Am. Vol.26, pp 984-989.

[15] Gates, E.M., 1977 (The influence of Free-Stream Turbulence, Free Stream Nuclei Populations and a Drag-reducing Polymer on Cavitation Inception on Two Axisymmetric Bodies California Institute of Technology, Rep. No. Eng 183-2.

[16] Harvey, E.N., McElroy, W.D., Whiteley, A.H., 1947 *On Cavity Formation in Water*, Journal of Applied Physics, Vol.18, pp162-172.

[17] Hoekstra, M., Vaz, G. *The Paartial Cavity on a @D Foil Revisited*, 7th Int. Conference on Cavitation CAV2009, Ann Arbor, Michigan, U.S.A.

[18] Holl, J.W., 1960, *An Effect of Air Content on the Occurrence of Cavitation*, Trans. A.S.M.E., Journal of Basic Eng. Vol.82, pp941-946.

[19] Holl, J.W., Carrol, J.A., 1981, *Observations of the Various Types of Limited Cavitation on Axisymmetric Bodies*, PUB A.S.M.E. Journal of Fluids Eng.,Vol 103,pp415-423

[20] Huang, T.T., 1981, *Cavitation Inception Observations on Six Axisymmetric Headforms*, A.S.M.E. Journal of Fluids Engineering, Vol 103,PP273-278

[21] ITTC, 1978,Proceedings 15th ITTC, The Haque, Report of the Performance Committee.

[22] Johnsson, C.A., Hsieh,T., 1966, *The Influence of Trajectories of Gas Nuclei on Cavitation Inception*, 6th Symposium on Naval Hydrodynamics, Washington D.C., pp163-178.

[23] Takagi,K., Kato,H.,Kato,D.,Sugimoto, A., 2006, *Destruction of Plankton by Two-Dimensional Cavitating Jet*, Sixth International Symposium on Cavitation CAV2006, Wageningen, The Netherlands.

[24] Keller, A.P., 1974 *Investigations Concerning Scale Effects of the Inception of Cavitation*, Proc. I.Mech.Eng. Conference on Cavitation, Edinburgh, 109-117.

[25] KLEBANOFF, P.S., SCHUBAUER, G.B., TIDSTROM,K.D., 1955, *Measurements of the Effect of Two-dimensional and Three-dimensional Roughness Elements on Boundary Layer Transition*, J. Aeron. Sciences

[26] Knapp, R.T., Hollander, A., 1948, *Laboratory Investigations of the Mechanism of Cavitation*, Trans. A.S.M.E., Vol.70, pp.419-435.

[27] Knapp, R.T., Daily, J.W., Hammitt, F.G., 1970, *C*avitation, New York : McGraw-Hill.

[28] Knapp, R.T., Hollander, A., 1948, *L*aboratory Investigations of the Mechanism of Cavitation, Trans. A.S.M.E., Vol 70, pp419-435.

[29] Korkut, E., Atlar, M., 2000, *On the Importance of Effect of Turbulence in Cavitation Inception Tests of Marine Propellers*, Proceedings of Royal Society of London A: Mathematical, Physical and Engineering Sciences, Vol.458 , pp.29-48.

[30] Kreider, W., Crum, L., Bailey,M., Matula, T.,Khoklova, V., Sapozhnikov,O., 2006, *Acoustic Cavitation and Medical Ultrasound*,Sixth International Symposium on Cavitation CAV2006, Wageningen, The Netherlands.

[31] Kumar, S., Brennen, C.E., 1996, *A Study of Pressure Pulses generated by Travelling Bubble Cavitation*, Journal of Fluid Mechanics Vol 255 pp541.

[32] Hwansung Lee, Tomonori Tsukiya, Akihiko Homma, Tadayuki Kamimura,Eisuke Tatsumi, Yoshiyuki Taenaka, Hisateru Takano, *Observation of Cavitation in a Mechanical Heart Valve*, Fifth International Symposium on Cavitation (cav2003),Osaka, Japan.

[33] Kuiper, G., 1978, *Scale Effects on Propeller Cavitation*, 12th Symposium on Naval Hydrodynamics, Washington D.C., USA.

[34] Kuiper, G. 1981, *Cavitation Inception on Ship Propeller Models*, Thesis Technical University Delft.

[35] Kuiper, G. 2008, *Fundamentals of Ship Resistance and Propulsion*, Course Lectures Technical University Delft.

[36] Landa, E.R., Nimmo, J.R.,2003 *The Life and Scientific Contributions of Lyman J. Briggs*, Journal of the Soil Science Society of America, Vol 67 no 3, pp 681-693. http://soil.scijournals.org/cgi/reprint/67/3/681

[37] Ligtelijn, J.T., van der Kooij, J., Kuiper, G., van Gent,W., 1992, *Research on Propeller-Hull Interaction in the Depressurized Towing Tank*, Hydrodynamics, Computations,Model Tests and Reality (Marin), Elseviers Science Publishers.

[38] Morch E.M., 2000, Paper on Cav2003.

[39] Moerch, K.A. 2009, *C*avitation Nuclei: Experiment and Theory,Journal of Hydrodynamics Vol21 p176.

[40] Neppiras, E.A., Noltink, B.E., 1951, *Cavitation produced by Ultrasonics*, Proc. Phys. Soc. London, pp 1032-1038.

[41] Ohl, C-D., Arora, M. ,Roy, I., Delius. M., Wolfrum, B.,2003, *Drug Delivery Following Shock Wave Induced Cavitation* , Fifth International Symposium on Cavitation (cav2003),Osaka, Japan.

[42] Plesset, M.S., 1949, *The Dynamics of Cavitation Bubbles*, ASME Journal of Appl. Mech. 1949, pp 277-232.

[43] Schiebe, F.R., 1972, *Measurement of the Cavitation Susceptibility of Water using Standard Bodies*, St. Anthony Fall Hydraulic Lab, Univ. of Minnesota, report 118.

[44] Schlichting, H., 1968, *Boundary Layer Theory*, McGraw-Hill, 6th edition.

[45] Terwisga, T.J.C., Fitzsimmons, P.A., Li,Z., Foeth, E-J. *Cavitation Erosion-A review of Physical Mechanisms and Erosion Risk Models*, 7th International Symposium on Cavitation, CAV2009, Ann Arbor, Michigan, U.S.A.

[46] Jin Wang, 2009, *Nozzle-geometry-dependent breakup of diesel jets by ultrafast x-ray imaging: implication of in-nozzle cavitation*, Seventh Int. Symp. on Cavitation: CAV2009, Ann Arbor, Michigan, U.S.A.

[47] Watanabe, S., Furukawa, A., Yoshida, Y., Tsujimoto, Y., 2009, *Analytical investigations of thermodynamic effect on cavitation characteristics of sheet and tip leakage vortex cavitation*, Seventh Int. Symp. on Cavitation: CAV2009, Ann Arbor, Michigan, USA.

[48] Williams,M., Kawakami, E., Amromin, E., Arndt,R. *Effects of Surface Characteristics on Hydrofoil Cavitation*, Seventh Int. Symp. on Cavitation: CAV2009, Ann Arbor, Michigan, USA.

[49] Yoshimura,T., Kubota, S., Seo, T., Sato,K., 2009, *Development of Ballast Water Treatment Technology by Mechanochemical Cavitations*,Seventh Int. Symp. on Cavitation: CAV2009, Ann Arbor, Michigan, USA.

[50] Yount, D.E. 1979, *S*kins of Varying Permeability: A Stabilization Mechanism For Gas Cavitation Nuclei,A. ACCOUST. SOC. AM. 65(6).

Appendix A

Air Content of Water

The amount of air dissolved in water α can be expressed in many ways. The most common ways in literature are

- the gas fraction in weight ratio α_w

- the gas fraction in volume ratio α_v

- the molecule ratio

- the saturation rate

- the partial pressure of air

A.1 Solubility

Air is a mixture of 21 percent oxygen, 78 percent nitrogen and one percent of many other gases, which are often treated as nitrogen. The specific mass of gases involved in air are:

Oxygen (O_2)	1.429	kg/m^3
Nitrogen (N_2)	1.2506	kg/m^3
Air	1.292	kg/m^3

The maximum amount of gas that can be dissolved in water, the solubility), depends on pressure and temperature. It decreases with increasing temperature and increases with increasing pressure. The solubility of oxygen in water is higher than the solubility of nitrogen. Air dissolved in water contains approximately 36 percent oxygen compared to 21 percent in air.The remaining amount can be considered as Nitrogen. Nuclei which are in equilibrium with saturated water therefore contain 36 percent oxygen. But nuclei which are generated from the air above the water contain 21 percent oxygen. Since the ratio between oxygen and nitrogen is not fixed, it is difficult to relate measurements of dissolved oxygen (by osmose) to measurements of dissolved air (from e.g a van Slijke apparatus).

The amount of oxygen dissolved in water at atmospheric pressure at 15 degrees Celcius is approximately $10*10^-6 kg/kg$. For nitrogen this value is about $15*10^-6$, so the solubility of air in water is the sum of both: $25*10^-6$. Here the dissolved gas contents are expressed as a weigth ratio α_w.Air is very light relative to water and the weight ratio is very small. This ratio is therefore often expressed as parts per million (in weight), which is $10^6*\alpha_w$.

A.2 The Gas Fraction in Volume Ratio

The volume of gas dissolved per cubic meter of water depends on temperature and pressure. Therefore this volume ratio is expressed in *standard conditions* of 0 degrees Celcius and 1013 mbar (atmospheric conditions). The dependency of the volume of water on temperature and pressure is neglected. The volume of the dissolved air is then described by the law of Boyle-Gay-Lussac:

$$\frac{p * Vol}{273 + T} = constant \qquad (A.1)$$

The volume fraction at (p,T) can be related to the volume fraction in standard conditions:

$$\alpha_v = \alpha_v(p, T)\frac{273p}{(273 + T)1013} \qquad (A.2)$$

The gas fraction in volume ratio is dimensionless (m^3/m^3). Be careful because sometimes this is violated by using cm^3/l $(1000*\alpha_v)$ or parts per million (ppm) which is $10^6 * \alpha_v$.

α_v is found from α_w by:

$$\alpha_v = \frac{\rho_{water}}{\rho_{air}}\alpha_w \qquad (A.3)$$

in which ρ is the specific mass in kg/m^3. At 15 deg. Celcius and 1013 mbar pressure the specific mass of water $\rho_w = 1000 kg/m^3$ and the specific mass of air is $1.223 kg/m^3$, so for air $\alpha_v = 813\alpha_w$.

A.3 The Gas Fraction in Molecule ratio

The dissolved amount of gas can also be expressed as the ratio in moles(Mol/Mol). Molar masses may be calculated from the atomic weight in combination with the molar mass constant (1 g/mol) so that the molar mass of a gas or fluid in grams is the same as the atomic weight.
The molar ratio α_m is easily found from the weight ratio by

$$\alpha_w = \alpha_m\frac{M_{(water)}}{M_{(gas)}} \qquad (A.4)$$

in which M is the molar weight, which is 18 for water, 16 for oxygen(O_2) and 28 for Nitrogen (N_2). For air a virtual molar weigth can

be defined using the ratio of oxygen and nitrogen of 21/79 this virtual molar weight of air is about 29.

A.4 The saturation rate

The saturation rate is the amount of gas in solution as a fraction of the maximum amount that can go in solution in the same conditions. Since the saturation rate is dimensionless. It is independent of the way in which the dissolved gas or the solubility is expressed. The saturation rate is important because it determines if and in which direction diffusion will occur at a free surface. The saturation rate varies with temperature and pressure, mainly because the solubility of gas changes with these parameters.

A.5 The partial pressure

Sometimes the amount of dissolved gas is expressed as the partial pressure of the gas (mbar or even in mm HG). This is based on Henry's law, which states that the amount of gas dissolved in a fluid is proportional to the partial pressure of that gas. In a van Slijke apparatus a specific volume of water is taken and subjected to repeated spraying in near vacuum conditions (a low pressure decreases the solubility). This will result in collecting the dissolved in a chamber of specific size. By measuring the pressure in that chamber the amount of dissolved gas is found. Note that this pressure is not directly the partial pressure. A calibration factor is required which depends on the apparatus.

Appendix B

Standard Cavitators

A standard cavitator is a reference body which can be used to compare and calibrate cavitation observations and measurements. Its geometry has to be reproduced accurately and therefore an axisymmetric headform has been used as a standard cavitatior.

Such an axisymmetric body has been investigated in the context of the ITTC (International Towing Tank Conference).This is a worldwide conference consisting of towing tanks (and cavitation tunnels) which have the goal of predicting the hydrodynamic behavior of ships. To do that model tests and calculations are used. They meet every three years to discuss the state of the art and to define common problem areas which have to be reviewed by committees. The ITTC headform has a flat nose and an elliptical contour [22]. Its characteristics are given in Fig B.1.

This headform has been used to compare cavitation inception conditions and cavitation patterns in a range of test facilities. The results showed a wide range of inception conditions and also a diversity of cavitation patterns in virtually the same condition, as illustrated in Fig B.3. This comparison lead to the investigation of viscous effects on cavitation and cavitation inception.

The simplest conceivable body to investigate cavitation is the hemispherical headform. This is an axisymmetric body with a hemispere as the leading contour. Its minimum pressure coefficient is -0.74. The hemisperical
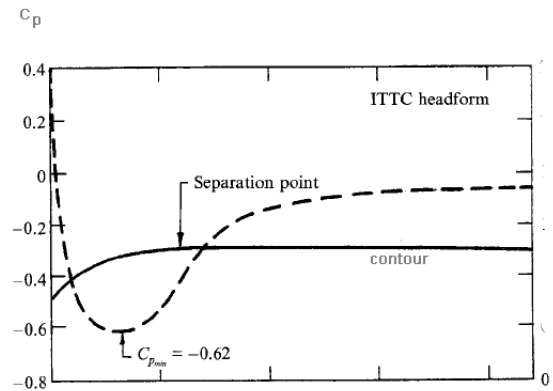
Figure B.1: Contour and Pressure Distribution on the ITTC Headform [31]

headform was used to compare inception measurements in various cavitation tunnels. However, it was realized later on that the boundary layer flow on both the ITTC and on the hemisperical headform was not as simple as the geometry suggested. In most cases the Reynolds numbers in the investigations was such that the boundary layer over the headform remained laminar and the pressure distribution was such that a laminar separation bubble occurred, in the position indicated in Fig. B.1. This caused viscous effects on cavitation inception and made the headform less suitable as a standard body. Note that the location of laminar separation is independent of the Reynolds number. When the Reynolds number becomes high transition to turbulence occurs upstream of the sep-

71
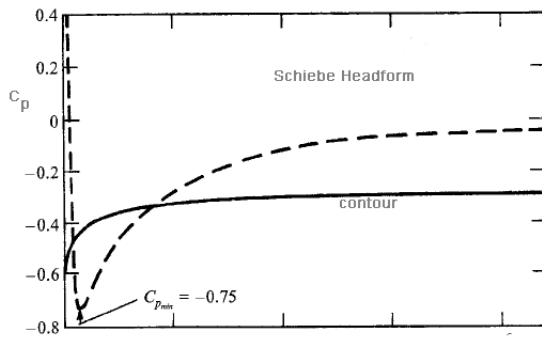
Figure B.2: Contour and Pressure Distribution of the Schiebe body [31]

aration location and separation will disappear.

To avoid laminar separation another headform was developed by Schiebe ([43]) and this headform bears his name ever since. The contour and pressure distribution on the Schiebe headform are given in Fig. B.2. This headform has no laminar separation and transition to a turbulent boundary layer will occur at a location which depends on the Reynolds number.

Many other headform shapes have been investigated with different minimum pressure coefficients and pressure recovery gradients.(e.g.[20])
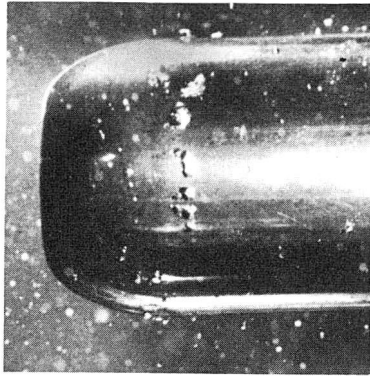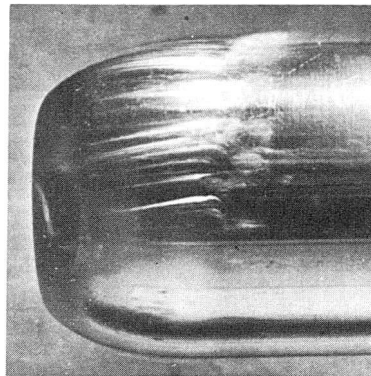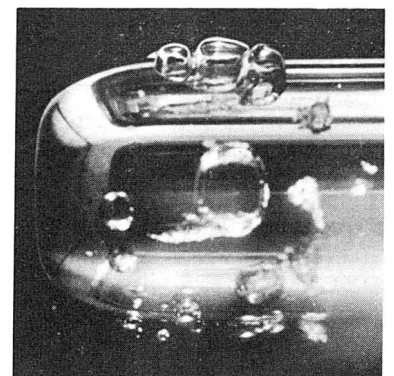
1. Rome   2. AEW   3. Delft
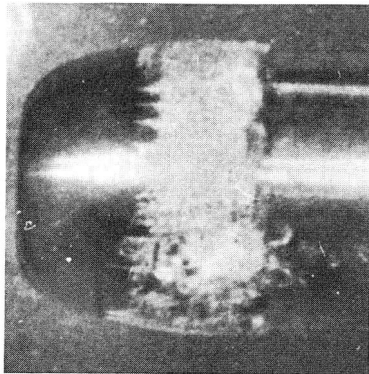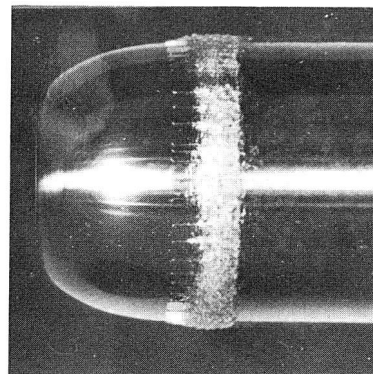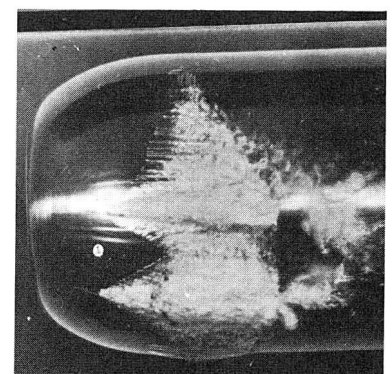
4. NPL   5. Cal. Tech.   6. Cal. Tech.
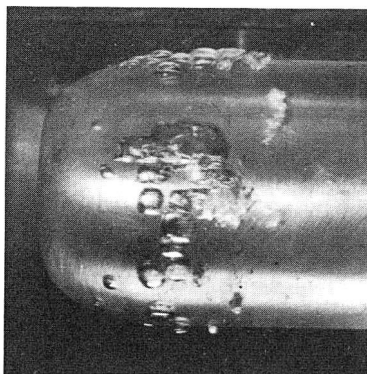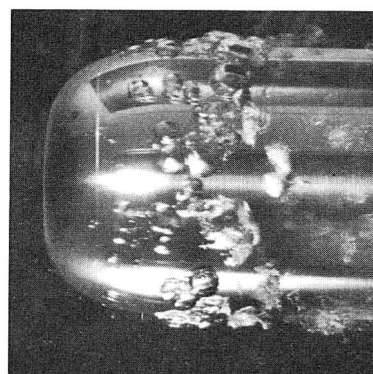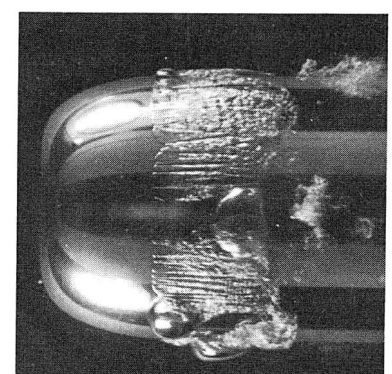
7. SSPA   8. SSPA   9. SSPA

Figure B.3: Comparative measurements of cavitation inception on the ITTC headform
source:ITTC

Appendix C

Tables

T	p_v
Celcius	N/m^2
0	608.012
2	706.078
4	813.951
6	932
8	1069
10	1226
12	1402
14	1598
15	1706
16	1814
18	2059
20	2334
22	2638
24	2981
26	3364
28	3785
30	4236
32	4756
34	5315
36	5943
38	6619
40	7375

Table C.1: Vapor pressure of Water.

Temp. deg. C.	kinem. visc. fresh water $m^2/sec \times 10^6$	kinem. visc. salt water $m^2/sec \times 10^6$
0	1.78667	1.82844
1	1.72701	1.76915
2	1.67040	1.71306
3	1.61665	1.65988
4	1.56557	1.60940
5	1.51698	1.56142
6	1.47070	1.51584
7	1.42667	1.47242
8	1.38471	1.43102
9	1.34463	1.39152
10	1.30641	1.35383
11	1.26988	1.31773
12	1.23495	1.28324
13	1.20159	1.25028
14	1.16964	1.21862
15	1.13902	1.18831
16	1.10966	1.15916
17	1.08155	1.13125
18	1.05456	1.10438
19	1.02865	1.07854
20	1.00374	1.05372
21	0.97984	1.02981
22	0.95682	1.00678
23	0.93471	0.98457
24	0.91340	0.96315
25	0.89292	0.94252
26	0.87313	0.92255
27	0.85409	0.90331
28	0.83572	0.88470
29	0.81798	0.86671
30	0.80091	0.84931

Table C.2: Kinematic viscosities adopted by the ITTC in 1963

R_n	$C_f \times 10^3$
1×10^5	8.333
2	6.882
3	6.203
4	5.780
5	5.482
6	5.254
7	5.073
8	4.923
9	4.797
1×10^6	4.688
2	4.054
3	3.741
4	3.541
5	3.397
6	3.285
7	3.195
8	3.120
9	3.056
1×10^7	3.000
2	2.669
4	2.390
6	2.246
8	2.162
1×10^8	2.083
2	1.889
4	1.721
6	1.632
8	1.574
1×10^9	1.531
2	1.407
4	1.298
6	1.240
8	1.201
1×10^{10}	1.17x

Table C.3: Friction coefficients according to the ITTC57extrapolator.

Temp. deg. C.	density fresh water kg/m^3	density salt water kg/m^3
0	999.8	1028.0
1	999.8	1027.9
2	999.9	1027.8
3	999.9	1027.8
4	999.9	1027.7
5	999.9	1027.6
6	999.9	1027.4
7	999.8	1027.3
8	999.8	1027.1
9	999.7	1027.0
10	999.6	1026.9
11	999.5	1026.7
12	999.4	1026.6
13	999.3	1026.3
14	999.1	1026.1
15	999.0	1025.9
16	998.9	1025.7
17	998.7	1025.4
18	998.5	1025.2
19	998.3	1025.0
20	998.1	1024.7
21	997.9	1024.4
22	997.7	1024.1
23	997.4	1023.8
24	997.2	1023.5
25	996.9	1023.2
26	996.7	1022.9
27	996.4	1022.6
28	996.2	1022.3
29	995.9	1022.0
30	995.6	1021.7

Table C.4: Densities as adopted by the ITTC in 1963.

Appendix D

Nomenclature

ρ	density of water	$\frac{kg}{m^3}$	See TableC.4
C_g	gas concentration	kg/m^3	see Appendix A
D_g	diffusion coefficient	m^2/sec	representative value $2 * 10_9$
D	diameter	m	
F_d	drag	N	
g	acceleration due to gravity	$\frac{m}{sec^2}$	Taken as 9.81
Nd	number density of nuclei	m^-4	
p_g	gas pressure	$fracNm^2$	
$fracNm^2$			
p_v	equilibrium vapor pressure		
R	radius	m	
μ	dynamic viscosity of water	$\frac{kg}{m*sec}$	
ν	kinematic viscosity of water	$\frac{m^2}{sec}$	$(\nu = \frac{\mu}{\rho})$See Table C.2
s	surface tension	Nm	for water 0.075